Applied Mathematics & Information Sciences
An International Journal

http://dx.doi.org/10.18576/amis/120302

Unsteady MHD Flow of Non-Newtonian Fluid in a Channel Filled with a Saturated Porous Medium with Asymmetric Navier Slip and Convective Heating

Lazarus Rundora[1,*] *and Oluwole D. Makinde*[2]

[1] Department of Mathematics and Applied Mathematics, University of Limpopo, Turfloop Campus, Private Bag X1106 Sovenga 0727, South Africa
[2] Faculty of Military Science, Stellenbosch University, Private Bag X2 Saldanha 7395, South Africa

Received: 9 Jul. 2016, Revised: 12 Mar. 2018, Accepted: 31 Mar. 2018
Published online: 1 May 2018

Abstract: This paper aims to computationally study the effects of Navier slip on an unsteady hydromagnetic flow of a pressure driven, reactive, variable viscosity, electrically conducting third-grade fluid through a porous saturated medium with asymmetrical convective boundary conditions. It is assumed that the chemical kinetics in the flow system is exothermic and that the asymmetric convective heat exchange with the surrounding medium at the surfaces follows Newtons law of cooling. The coupled nonlinear partial differential equations governing the flow and heat transfer are derived and solved numerically using a semi-implicit finite difference scheme. The flow and heat transfer characteristics are analyzed graphically and discussed for different values of the parameters embedded in the system. It is observed that the lower wall slip parameter increases the fluid velocity profiles. The upper wall slip parameter is seen to retard the velocity profiles while it increases the fluid temperature profiles. The wall slip parameters increase the skin friction and the Nusselt number. The wall slip parameters as well as the variable viscosity parameter, the viscous heating parameter and the numerical exponent m reduce the thermal criticality values of the reaction parameter.

Keywords: Unsteady MHD flow, porous medium, third grade fluid, Navier slip, convective heating, finite difference method

1 Introduction

Research interest in studies of phenomena connected with convective hydromagnetic fluid flow has gathered momentum in recent times, and it is reasonable to pin down the interest on the broad applications of the field in science, engineering and technology. Hydromagnetic fluid flow studies were pioneered by Hartmann[1], and following his ground breaking work the rheological community has undertaken to investigate hydromagnetic fluid flow and heat transfer in different geometries under varied physical effects. The flow of electrically conducting viscous fluid between two parallel plates in the presence of a transversely applied magnetic field has applications in many devices and processes such as magnetohydrodynamic (MHD) power generators, MHD pumps, accelerators, aerodynamics heating, electrostatic precipitation, polymer technology, petroleum industry, cooling of nuclear reactors, geothermal energy extraction, metal purification, etc. See [2,3,4,5]. Some of the most recent studies were undertaken in [6,7,8,9,10]. Studies have also, to a greater extent, tended to focus on the flow of fluids that exhibit non-Newtonian character. Fluids such as drilling muds, hydrocarbon oils, polyglycols, synthetic esters, polyphenylethers, oil and greases, clay coating and suspensions, paper products, food stuffs and slurries exhibit behavioural features that cannot be explained by the Navier-Stokes model [11,12,13,14]. Among the models that have been suggested in trying to explain such non-Newtonian character are the fluids of differential type exemplified by the fluids of third grade. Detailed studies of the mechanics of fluids of the differential type are found in [15,16]. [17] studied convection heat and mass transfer in a hydromagnetic flow of a second grade fluid past a semi-infinite stretching sheet in the presence of thermal radiation and thermal diffusion.

* Corresponding author e-mail: lazarus.rundora@ul.ac.za

Meanwhile in most studies the assumption of the no-slip boundary condition, namely the fluid velocity relative to the solid is zero on the fluid-solid interface [18], has become the norm. This is despite the fact that the no-slip boundary condition is a hypothesis rather than a condition deduced from any principle. It is owing to this fact that its validity has been debated in scientific literature [19]. Evidences of slip of a fluid on a solid surface were reported by several authors, see for example, [20,21]. Studies involving flow and heat transfer in channels with wall slip are important as they lead to the improvement of design and operation of many industrial and engineering devices.

This study is an investigation of the effects of Navier slip on unsteady hydromagnetic flow of a reactive variable viscosity, electrically conducting third-grade fluid through a porous saturated medium with asymmetrical convective boundary conditions. The rest of the paper is organized as follows: in section 2, mathematical model formulation is presented, the solution process (a semi-implicit finite difference scheme) is implemented in section 3, and numerical and graphical results as well as their discussion are given in section 4.

2 Mathematical Formulation

An unsteady flow of an incompressible electrically conducting, third-grade, variable viscosity, and reactive fluid through a channel filled with a homogeneous and isotropic porous medium is considered. It is assumed that the flow is subjected to the influence of an externally applied homogeneous magnetic field as depicted in (Figure 1). The fluid has small electrical conductivity so that the electromagnetic force produced has small magnitude. The plate surfaces are subjected to asymmetric convective heat exchange with the ambient due to unequal heat transfer coefficients and the fluid motion is induced by an applied axial pressure gradient. We choose the $\overline{x}$-axis parallel to the channel and the $\overline{y}$-axis normal to it. Under the above assumptions, and neglecting the reacting viscous fluid consumption, the governing equations for the momentum and heat balance are formulated as in [22,23,24,25,26], and can be written as;

$$\rho\frac{\partial u}{\partial \overline{t}} = -\frac{\partial \overline{P}}{\partial \overline{x}} + \frac{\partial}{\partial \overline{y}}\left[\overline{\mu}(T)\frac{\partial u}{\partial \overline{y}}\right] + \alpha_1\frac{\partial^3 u}{\partial \overline{y}^2\partial \overline{t}} + 6\beta_3\frac{\partial^2 u}{\partial \overline{y}^2}\left(\frac{\partial u}{\partial \overline{y}}\right)^2 - \frac{\overline{\mu}(T)u}{\rho K} - \sigma B_0^2 u, \quad (1)$$

$$\rho c_P\frac{\partial T}{\partial \overline{t}} = k\frac{\partial^2 T}{\partial \overline{y}^2} + \sigma B_0^2 u^2 + \left(\frac{\partial u}{\partial \overline{y}}\right)^2\left(\overline{\mu}(T) + 2\beta_3\left(\frac{\partial u}{\partial \overline{y}}\right)^2\right) + \frac{\overline{\mu}(T)u^2}{K} + QC_0A\left(\frac{hT}{\upsilon l}\right)^m e^{-\frac{E}{RT}}. \quad (2)$$

The appropriate initial and boundary conditions are

$$u(\overline{y},0) = 0, \quad T(\overline{y},0) = T_0, \quad (3)$$

$$\beta_0 u(0,\overline{t}) = \overline{\mu}(T)\frac{\partial u}{\partial \overline{y}}(0,\overline{t}),$$

$$-k\frac{\partial T}{\partial \overline{y}}(0,\overline{t}) = h_1\left[T_a - T(0,\overline{t})\right], \quad (4)$$

$$\beta_1 u(a,\overline{t}) = \overline{\mu}(T)\frac{\partial u}{\partial \overline{y}}(a,\overline{t}),$$

$$-k\frac{\partial T}{\partial \overline{y}}(a,\overline{t}) = h_2\left[T(a,\overline{t}) - T_a\right]. \quad (5)$$

where T_0 is the initial fluid temperature. The temperature dependent viscosity ($\overline{\mu}$) can be expressed as

$$\overline{\mu}(T) = \mu_0 e^{-b(T-T_0)}, \quad (6)$$

where b is a viscosity variation parameter and μ_0 is the initial fluid dynamic viscosity at temperature T_0. The dimensionless form of Eqns. (1) to (6)are:

$$\frac{\partial w}{\partial t} = G - Ha^2 w - S^2 w e^{-\alpha\theta} + e^{-\alpha\theta}\frac{\partial^2 w}{\partial y^2} - \alpha e^{-\alpha\theta}\frac{\partial\theta}{\partial y}\frac{\partial w}{\partial y} + \delta\frac{\partial^3 w}{\partial y^2\partial t} + 6\gamma\frac{\partial^2 w}{\partial y^2}\left(\frac{\partial w}{\partial y}\right)^2 \quad (7)$$

$$Pr\frac{\partial\theta}{\partial t} = \frac{\partial^2\theta}{\partial y^2} + \lambda\left[(1+\varepsilon\theta)^m exp\left(\frac{\theta}{1+\varepsilon\theta}\right)\right] + \lambda\Omega\left(Ha^2 w + S^2 w^2 e^{-\alpha\theta}\right) + \lambda\Omega\left[\left(\frac{\partial w}{\partial y}\right)^2\left(e^{-\alpha\theta} + 2\gamma\left(\frac{\partial w}{\partial y}\right)^2\right)\right], \quad (8)$$

$$w(y,0) = 0, \quad \theta(y,0) = 0 \quad (9)$$

$$w(0,t) = n_1 e^{-\alpha\theta(0,t)}\frac{\partial w}{\partial y}(0,t),$$

$$\frac{\partial\theta}{\partial y}(0,t) = -Bi_1[\theta_a - \theta(0,t)] \quad (10)$$

$$w(1,t) = n_2 e^{-\alpha\theta(1,t)}\frac{\partial w}{\partial y}(1,t),$$

$$\frac{\partial\theta}{\partial y}(1,t) = -Bi_2[\theta(1,t) - \theta_a], \quad (11)$$

where

$$y = \frac{\overline{y}}{a}, \quad \alpha = \frac{bRT_0^2}{E}, \quad w = \frac{\mu\rho a}{\mu_0},$$

$$\theta = \frac{E(T-T_0)}{RT_0^2}, \quad \theta_a = \frac{E(T_a-T_0)}{RT_0^2}, \quad \gamma = \frac{\beta_3\mu_0}{\rho^2 a^4},$$

$$\delta = \frac{\alpha_1}{\rho a^2}, \quad Bi_1 = \frac{h_1 a}{k}, \quad Bi_2 = \frac{h_2 a}{k},$$

$$Da = \frac{K}{a^2}, \quad Pr = \frac{\mu_0 c_P}{k}, \quad \varepsilon = \frac{RT_0}{E},$$

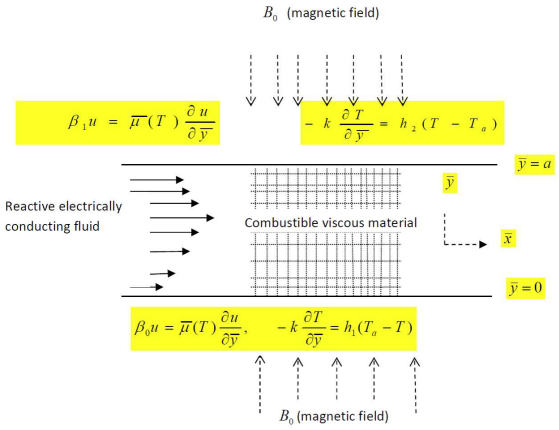

Fig. 1: Problem geometry and coordinate system

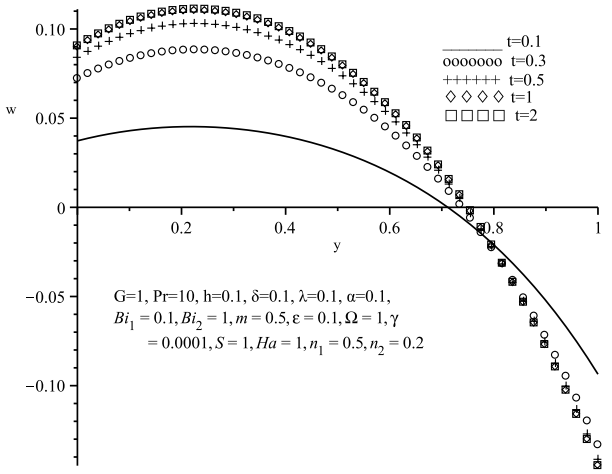

Fig. 2: Transient and steady state fluid velocity profiles

$$x = \frac{\overline{x}}{a},\ P = \frac{\overline{P}\rho a^2}{\mu_0^2},\ G = -\frac{\partial \overline{P}}{\partial \overline{x}},$$

$$S^2 = \frac{1}{Da},\ Ha^2 = \frac{\sigma B_0^2 a^2}{\mu_0},\ \mu = \frac{\overline{\mu}}{\mu_0},$$

$$\Omega = \left(\frac{\upsilon l}{hT_0}\right)^m \frac{\mu_0^3 e^{\frac{E}{RT}}}{\rho^2 QAa^4 C_0},\ t = \frac{\overline{t}\mu_0}{\rho a^2}$$

$$\lambda = \left(\frac{hT_0}{\upsilon l}\right)^m \frac{QEAa^2 C_0 e^{-\frac{E}{RT}}}{T_0^2 Rk},\ n_1 = \frac{\mu_0}{\beta_0 a},$$

$$n_2 = \frac{\mu_0}{\beta_1 a}$$

The skin friction (C_f) at the channel walls is given by

$$C_f = \frac{\rho\alpha^2\tau_w}{\mu_0^2} = e^{-\alpha\theta}\frac{dw}{dy}|_{y=0,1} \tag{12}$$

where $\tau_w = \overline{\mu}(T)\frac{\partial u}{\partial \overline{y}}$ is the shear stress evaluated at the wall $\overline{y} = 0, a$. The other dimensionless quantity of interest is the wall heat transfer rate (Nu) defined as

$$Nu = -\frac{d\theta}{dy}(1,t). \tag{13}$$

Eqns. (7)-(13) are solved using a semi-implicit finite difference scheme.

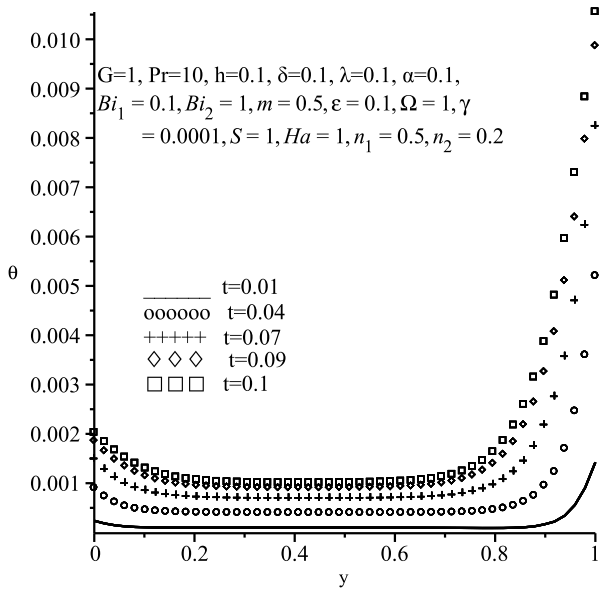

Fig. 3: Transient and steady state fluid temperature profiles

3 Numerical Solution

The semi-implicit finite difference scheme given in [27] is adopted. As in [28,29], implicit terms are taken at the intermediate time level $N + \xi$ where $0 \leq \xi \leq 1$. The discretization of the governing equations is based on a linear Cartesian mesh and uniform grid on which finite differences are taken. Both the second and first spatial derivatives are approximated by second-order central differences. The equations corresponding to the first and last grid points are modified to incorporate the boundary conditions. The semi-implicit scheme for the velocity component reads

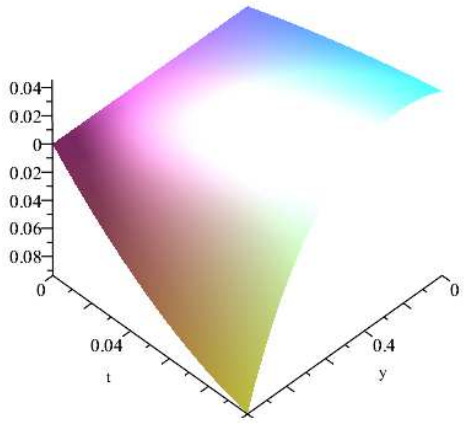

Fig. 4: Three dimensional representation of velocity field

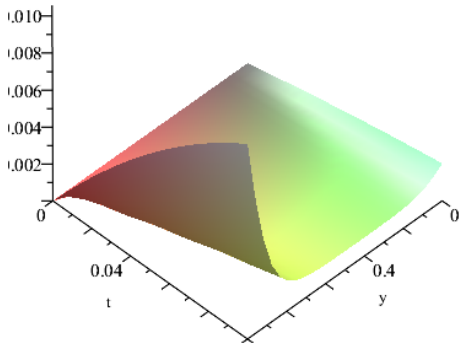

Fig. 5: Three dimensional representation of temperature field

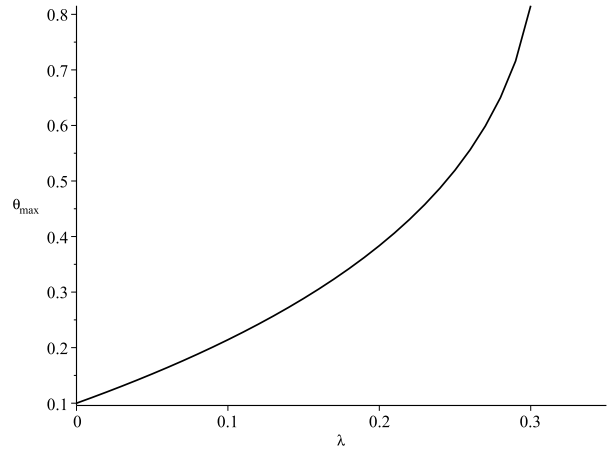

Fig. 6: Blow up of fluid temperature for large λ

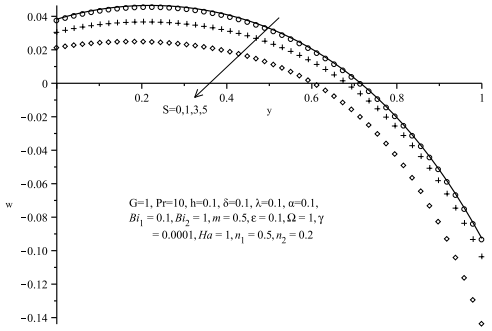

Fig. 7: Effects of the porous medium shape parameter, S, on fluid velocity profiles

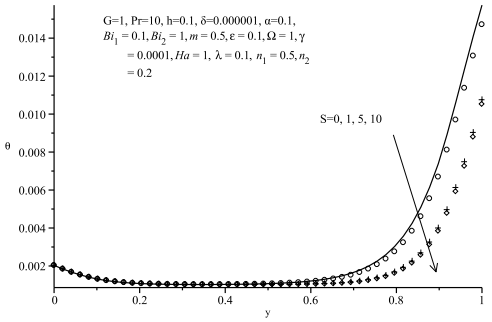

Fig. 8: Effects of the porous medium shape parameter, S, on fluid temperature profiles

$$\frac{\partial}{\partial t}\left(w-\delta\frac{\partial^2 w}{\partial y^2}\right) = G - S^2 e^{-\alpha\theta^{(N)}} w^{(N+\xi)} - Ha^2 w^{(N+\xi)} + e^{-\alpha\theta^{(N)}}\frac{\partial^2}{\partial y^2} w^{(N+\xi)} - \left[\alpha e^{-\alpha\theta}\frac{\partial\theta}{\partial y}\frac{\partial w}{\partial y}\right]^{(N)} + 6\gamma\left(\frac{\partial}{\partial y} w^{(N)}\right)^2 \frac{\partial^2}{\partial y^2} w^{(N+\xi)} \tag{14}$$

In Eqn. (14), it is understood that

$$\frac{\partial \square}{\partial t} := \frac{\left(\square^{(N+1)} - \square^{(N)}\right)}{\triangle t}$$

. The equation for $w^{(N+1)}$ then becomes

$$\begin{aligned} -r_1 w_{j-1}^{(N+1)} + r_2 w_{j-1}^{(N+1)} - r_1 w_{j+1}^{(N+1)} &= \triangle t G + (w + \delta w_{yy})^{(N)} \\ &- \alpha\triangle t\left(e^{-\alpha\theta}\theta_y \Gamma\right)^{(N)} \\ &- \triangle t S^2 e^{-\alpha\theta^{(N)}}(1-\xi) w^{(N)} \\ &- -\triangle t Ha^2 (1-\xi) w^{(N)} \\ &+ \triangle t(1-\xi)\left(e^{-\alpha\theta} + 6\gamma\Gamma^2\right)^{(N)} w_{yy}^{(N)} \end{aligned} \tag{15}$$

where

$$r_1 = \frac{1}{\triangle y^2}\left[\delta + \xi \triangle t\left(\mu + 6\gamma\Gamma^2\right)^{(N)}\right],$$

$$r_2 = \left(1 + \xi \triangle t S^2 \mu^{(N)} + \xi \triangle t Ha^2 + 2r_1\right),$$

with $\mu = exp(-\alpha\theta)$ and $\Gamma = w_y$. The solution procedure for $w^{(N+1)}$ thus reduces to inversion of tri-diagonal matrices, which is an advantage over a full implicit scheme. The semi-implicit integration scheme for the temperature equation is similar to that for the velocity component. Unmixed second partial derivatives of the temperature are treated implicitly:

$$Pr\frac{\theta^{(N+1)} - \theta^{(N)}}{\triangle t} = \frac{\partial^2 \theta^{(N+\xi)}}{\partial y^2} + \lambda\left[(1+\varepsilon\theta)^m exp\left(\frac{\theta}{1+\varepsilon\theta}\right)\right]^{(N)} + \lambda\Omega\left(Ha^2 w + S^2 w^2 e^{-\alpha\theta}\right)^{(N)} + \lambda\Omega\left[\left(\frac{\partial w}{\partial y}\right)^2\left(e^{-\alpha\theta} + 2\gamma\left(\frac{\partial w}{\partial y}\right)^2\right)^{(N)}\right] \quad (16)$$

The equation for $\theta^{(N+1)}$ thus becomes

$$-r\theta_{j-1}^{(N+1)} + (Pr+2r)\theta_j^{(N+1)} - r\theta_{j+1}^{(N+1)} = \theta^{(N)} + \triangle t(1-\xi)\theta_{yy}^{(N)} + \lambda\triangle t\left[(1+\varepsilon\theta)^m exp\left(\frac{\theta}{1+\varepsilon\theta}\right)\right]^{(N)} + \lambda\Omega\triangle t\left(Ha^2 w + S^2 w^2 e^{-\alpha\theta}\right)^{(N)} + \lambda\Omega\triangle t\left[\left(\frac{\partial w}{\partial y}\right)^2\left(e^{-\alpha\theta} + 2\gamma\left(\frac{\partial w}{\partial y}\right)^2\right)^{(N)}\right] \quad (17)$$

where $r = \dfrac{\xi\triangle t}{\triangle y^2}$. The solution procedure again reduces to inversion of tri-diagonal matrices. The schemes (15) and (17) were checked for consistency. For $\xi = 1$, these are first order accurate in time but second-order accurate in space. The schemes in [27] have $\xi = \frac{1}{2}$ which improves the accuracy in time to second order. We use $\xi = 1$ here so that we are free to choose larger time steps and still obtain convergence to the steady solutions.

4 Results and Discussion

Figure 2 and figure 3 show transient increases in velocity and temperature profiles respectively until steady state is reached. Negative velocity profiles indicate flow reversal at the wall due to velocity slip. The Biot number at the lower wall Bi_1 has been set less than the Biot number at the upper wall Bi_2 . This implies that more heat flows into the fluid from the ambient through the upper wall than the lower wall and thus the fluid temperature near the upper wall will always be higher than that near the lower wall. This feature will be observed in all the temperature figures. Three dimensional representations of the velocity and temperature profiles are displayed in figure 4 and figure 5 respectively.

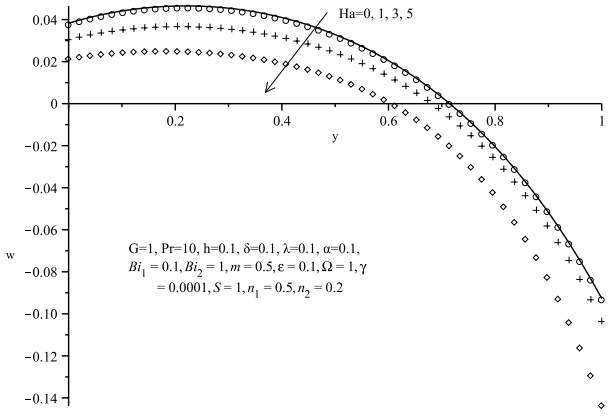

Fig. 9: Effects of the Hartmann number, Ha, on fluid velocity profiles

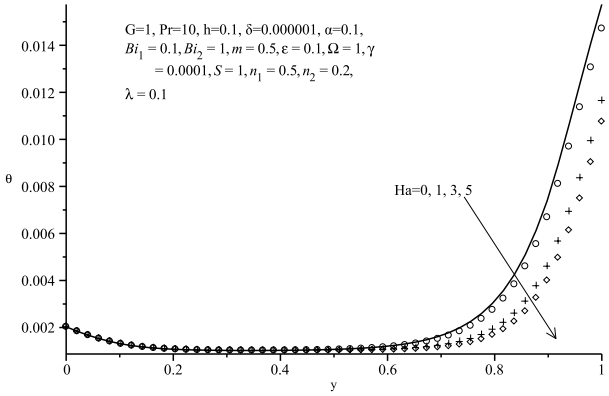

Fig. 10: Effects of the Hartmann number, Ha, on fluid temperature profiles

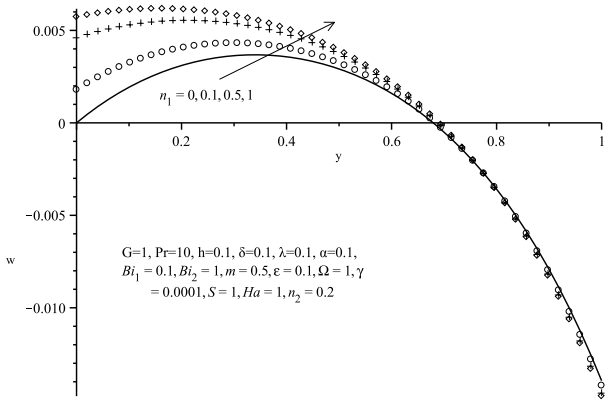

Fig. 11: Effects of the lower wall slip parameter, n_1, on fluid velocity profiles

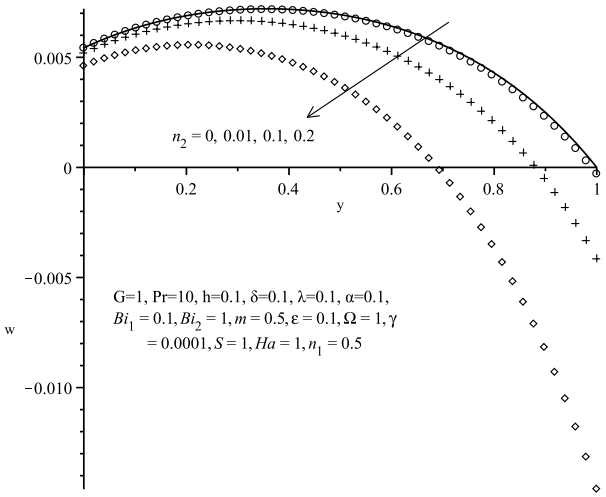

Fig. 12: Effects of the upper wall slip parameter, n_2, on fluid velocity profiles

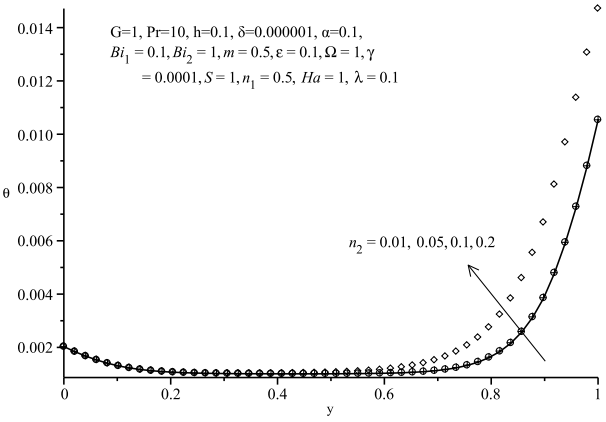

Fig. 13: Effects of the upper wall slip parameter, n_2, on fluid temperature profiles

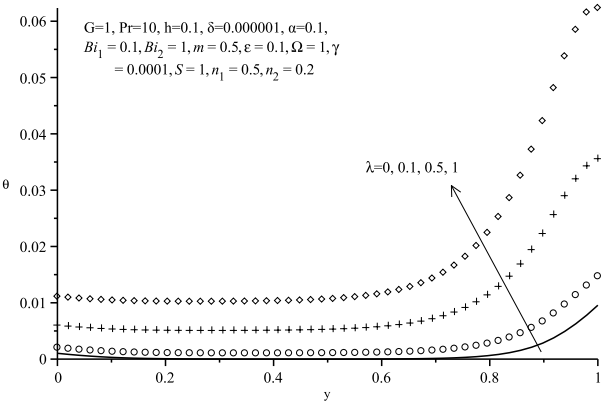

Fig. 14: Effects of the reaction parameter, λ, on fluid temperature profiles

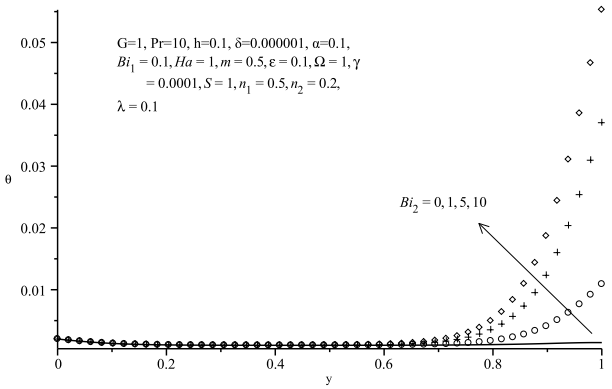

Fig. 15: Effects of the Biot number, Bi_2, on fluid temperature profiles

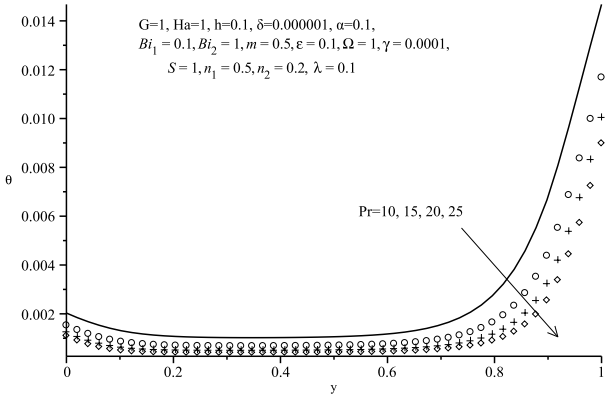

Fig. 16: Effects of the Prandtl number, Pr, on fluid temperature profiles

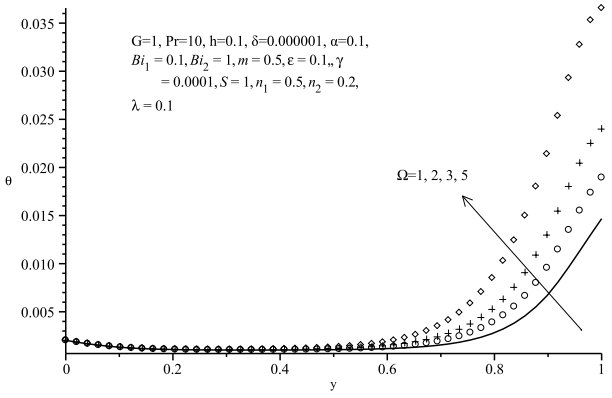

Fig. 17: Effects of the viscous heating parameter, Ω, on fluid temperature profiles

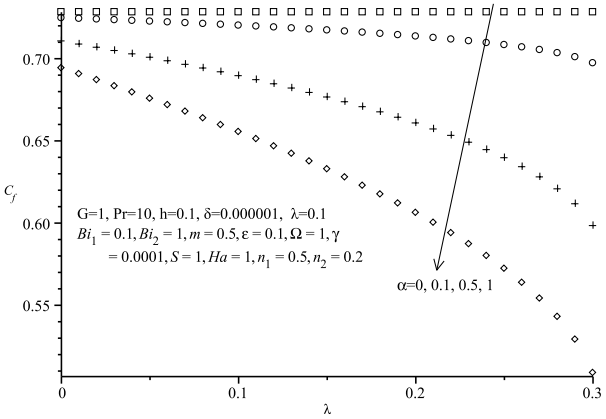

Fig. 18: Variation with λ and α of the wall shear stress, C_f

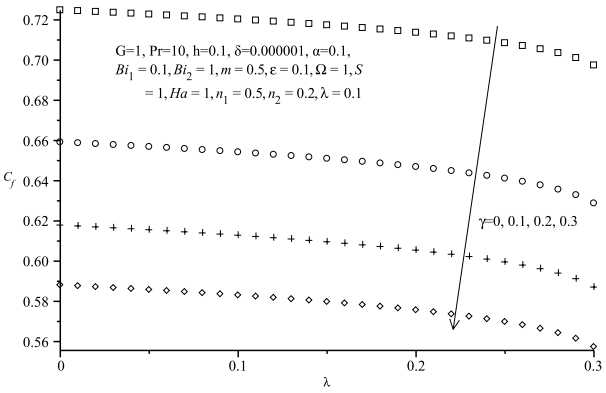

Fig. 19: Variation with λ and γ of the wall shear stress, C_f

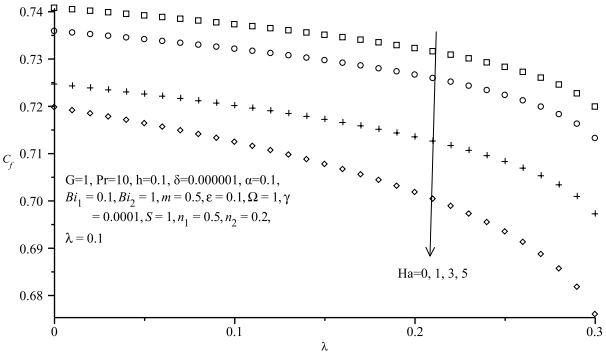

Fig. 20: Variation with λ and Ha of the wall shear stress, C_f

4.1 Blow-up of solutions

It is of paramount importance to know a priori which parameter value combinations help in maintaining stable optimum fluid temperature. Some parameter combination values, if un-monitored carefully, may lead to fluid

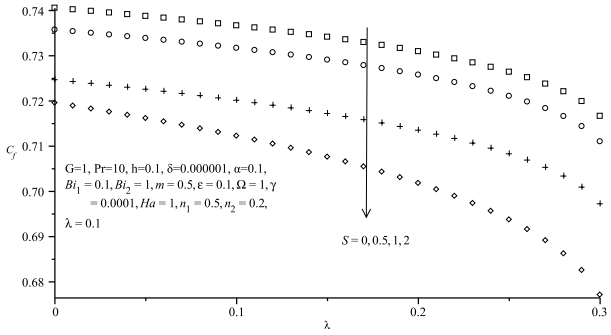

Fig. 21: Variation with λ and S of the wall shear stress, C_f

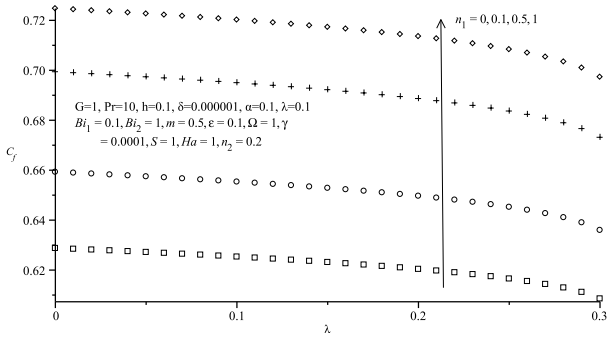

Fig. 22: Variation with λ and n_1 of the wall shear stress, C_f

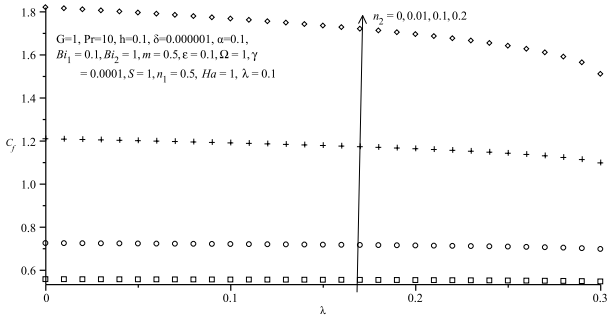

Fig. 23: Variation with λ and n_2 of the wall shear stress, C_f

temperature blow-up that may result in loss of life and property damage. In particular the value of the exothermic reaction parameter λ needs to be controlled as values larger than 0.3 lead to blow up of fluid temperature (figure 6).

4.2 Parameter dependence of solution

The higher the value of the porous medium parameter, S, the more complicated is the porous matrix and the more difficulty it is for the fluid particles to penetrate the

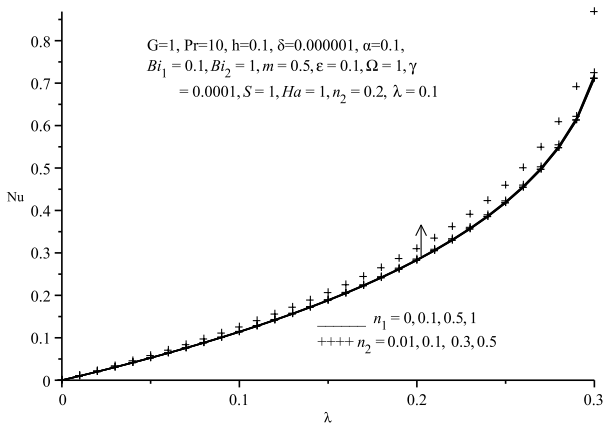

Fig. 24: Variation with λ and n_1, n_2 of the wall heat transfer rate, Nu

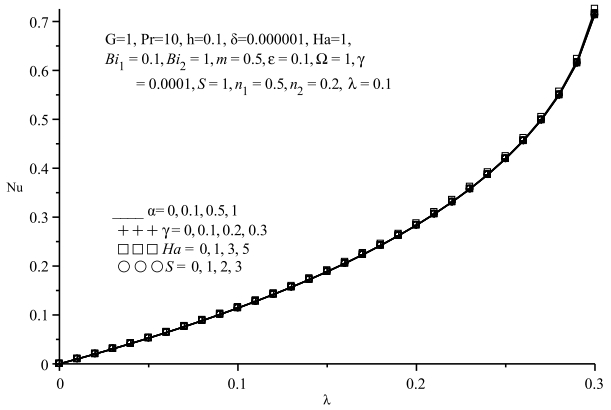

Fig. 25: Variation with λ and α, γ, Ha, S of the wall heat transfer rate, Nu

medium. In this way fluid velocity is diminished as the value of S increases. Figure 7 illustrates this behavior. As fluid velocity decreases, the viscous heating source terms in the temperature equation are reduced, and this causes a significant reduction in fluid temperature as depicted by figure 8. As figure 9 and figure 10 show, the effects of the Hartmann number, Ha , on velocity and temperature profiles mirror those of the porous medium parameter. Increasing the Hartmann number increases the damping effect of the externally applied magnetic field, and this damps the fluid flow.

From figure 11 and figure 12 we observe that the lower wall slip parameter, n_1 , increases the velocity of the fluid whereas on the contrary, the upper wall slip parameter, n_2 , diminishes the fluid velocity. It is the significant flow reversal at the upper wall due to velocity slip that causes retardation of the fluid velocity. The flow reversal at the upper wall causes rapid mixing of the fluid particles that in turn increases friction and this friction induces a temperature rise, (figure 13). The effect of the Frank-Kamenetskii parameter, λ, is to increase the rate of the exothermic chemical reaction. As λ increases the reaction rate increases and this inevitably causes the fluid temperature to rise, as depicted by figure 14. In fact, as the blow-up diagram (figure 6) shows, if this parameter is not controlled, explosions that can be harmful and fatal can occur.

An increase in the values of the Biot numbers Bi_1 and Bi_2 imply that heat flows by convection into the fluid from the ambient surrounding the channel walls. If Bi_1 is fixed and Bi_2 increases as in figure 15, it implies more heat flows into the fluid from the upper wall of the channel by convection and the fluid temperature near the upper wall increases. The model boundary conditions indicate the ambient temperature T_a is higher than that of the fluid inside the channel. Higher Prandtl numbers are generally associated with a decrease in fluid thermal conductivity. This is why figure 16 shows fluid temperature decreasing with increasing Prandtl numbers. The effects of the viscous heating parameter, Ω , (figure 17) on fluid temperature mirror those of the reaction parameter (figure 14).

4.3 Skin friction and Nusselt number

The physical quantities of engineering importance are the wall shear stress, C_f, and the wall heat transfer rate, Nu . Variation of the wall shear stress with the reaction parameter λ and the variable viscosity parameter, α, the non-Newtonian parameter, γ, the Hartmann number, Ha, and the porous medium parameter, S, is displayed in figures 18, 19, 20 and 21 respectively. Variation of the wall shear stress with λ and the lower and upper wall slip parameters n_1 and n_2 is shown in figure 22 and 23. The figures are plotted up to the solution blow-up values of the reaction parameter. It is observed that the variable viscosity parameter, the non-Newtonian parameter, the Hartmann number and the porous medium parameter have a diminishing effect on the wall shear stress. The wall slip parameters increase the wall shear stress.

Variation of the wall heat transfer rate with the reaction parameter λ and the variable viscosity parameter, α, the non-Newtonian parameter, γ, the Hartmann number, Ha, and the porous medium parameter, S, is displayed in figure 25. Variation of the wall heat transfer rate with λ and the lower and upper wall slip parameters n_1 and n_2 is shown in figure 24. The figures are also plotted up to the solution blow-up values of the reaction parameter. While it is clear from figure 24 that the upper wall slip parameter increases the wall heat transfer rate, the effects of the other parameters; the variable viscosity parameter, the non-Newtonian parameter, the Hartmann number, the porous medium parameter and the lower wall slip parameter on the Nusselt number are not clearly explained by the two figures. Table 1 is an attempt to describe the effects of these parameters on the Nusselt

number as well as to show computations of the thermal criticality values of λ , λ_c , as the parameters are varied. It has already been referred to earlier in this article that the need to control the reaction parameter is of crucial importance.

Table 1 shows that the thermal criticality values of the reaction parameter are increased by the porous medium parameter, the Hartmann number, the non-Newtonian parameter, the Biot number, Bi_2, and the activation energy parameter, ε. In other words, increasing the values of these parameters delays blow-up of solution which is a more desirable situation. On the other hand, the thermal criticality values of the reaction parameter are reduced by increasing the temperature dependent viscosity parameter, α, the numerical exponent, m, the viscous heating parameter,Ω, and the wall slip parameters n_1 and n_2. These parameters correspondingly increase the wall heat transfer rate and thus, accelerate solution blow-up.

Table 1: Thermal criticality values of λ for different parameter values

S	Ha	α	γ	Bi_2	m	ε	Ω	n_1	n_2	Nu	λ_c
0	1	0.1	0.1	1	0.5	0.1	1	0.5	0.2	0.877	0.296
1	1	0.1	0.1	1	0.5	0.1	1	0.5	0.2	0.849	0.296
2	1	0.1	0.1	1	0.5	0.1	1	0.5	0.2	0.843	0.297
3	1	0.1	0.1	1	0.5	0.1	1	0.5	0.2	0.858	0.299
1	1	0.1	0.1	1	0.5	0.1	1	0.5	0.2	0.849	0.296
1	3	0.1	0.1	1	0.5	0.1	1	0.5	0.2	0.854	0.299
1	4	0.1	0.1	1	0.5	0.1	1	0.5	0.2	0.861	0.297
1	1	0	0.1	1	0.5	0.1	1	0.5	0.2	0.917	0.297
1	1	0.5	0.1	1	0.5	0.1	1	0.5	0.2	0.854	0.295
1	1	1	0.1	1	0.5	0.1	1	0.5	0.2	0.874	0.293
1	1	0.1	0	1	0.5	0.1	1	0.5	0.2	0.875	0.296
1	1	0.1	0.2	1	0.5	0.1	1	0.5	0.2	0.889	0.297
1	1	0.1	0.3	1	0.5	0.1	1	0.5	0.2	0.871	0.297
1	1	0.1	0.1	1	0.5	0.1	1	0.5	0.2	0.849	0.296
1	1	0.1	0.1	2	0.5	0.1	1	0.5	0.2	0.840	0.400
1	1	0.1	0.1	3	0.5	0.1	1	0.5	0.2	0.693	0.400
1	1	0.1	0.1	1	-2	0.1	1	0.5	0.2	0.907	0.400
1	1	0.1	0.1	1	0	0.1	1	0.5	0.2	0.919	0.316
1	1	0.1	0.1	1	0.5	0.1	1	0.5	0.2	0.849	0.296
1	1	0.1	0.1	1	0.5	0	1	0.5	0.2	0.728	0.275
1	1	0.1	0.1	1	0.5	0.2	1	0.5	0.2	1.106	0.325
1	1	0.1	0.1	1	0.5	0.3	1	0.5	0.2	1.720	0.367
1	1	0.1	0.1	1	0.5	0.1	2	0.5	0.2	0.896	0.288
1	1	0.1	0.1	1	0.5	0.1	3	0.5	0.2	0.977	0.280
1	1	0.1	0.1	1	0.5	0.1	1	0.1	0.2	0.859	0.299
1	1	0.1	0.1	1	0.5	0.1	1	0.5	0.2	0.849	0.296
1	1	0.1	0.1	1	0.5	0.1	1	1	0.2	0.874	0.295
1	1	0.1	0.1	1	0.5	0.1	1	0.5	0.1	0.899	0.299
1	1	0.1	0.1	1	0.5	0.1	1	0.5	0.3	0.896	0.294
1	1	0.1	0.1	1	0.5	0.1	1	0.5	0.5	0.959	0.277

5 Conclusion

In this study, the effects of the Navier slip and other flow parameters on unsteady MHD reactive flow of a third-grade fluid through a porous saturated medium with asymmetric convective boundary conditions are investigated. It is concluded that the porous medium parameter and the Hartmann number retard the fluid velocity and temperature profiles. The lower wall slip parameter increases the fluid velocity profiles. The upper wall slip parameter diminishes the fluid velocity profiles and increases the fluid temperature. The skin friction is observed to be diminished by the porous medium parameter, the Hartmann number, the variable viscosity parameter and the non-Newtonian parameter. It is however, increased by the wall slip parameters. The wall slip parameters are also observed to increase the wall heat transfer rate and to reduce the thermal criticality values of the reaction parameter, λ. The temperature dependent viscosity parameter, the viscous heating parameter and the numerical exponent $m \in \{-2, 0, 0.5\}$ are also seen to play the same role.

Nomenclature

a - Channel width (m)
B_0 - Electromagnetic induction (tesla)
A - Rate constant
Bi - Biot number
c_P - Specific heat at constat pressure $(Jkg^{-1}K^{-1})$
Da - Darcy number
E - Activation energy (J)
G - Pressure gradient parameter
h - Boltzmann's constant (JK^{-1})
h_1, h_2 - Heat transfer coefficients at the lower and upper plates, respectively $(Wm^{-3}K^{-1})$
Ha - Hartmann number
k - Thermal conductivity $(Wm^{-1}K^{-1})$
K - Porous medium permeability (m^2)
l - Planck's number (Js)
$m \in \{-2, 0, 05\}$ - Numerical exponents for sensitised, Arrhenius and bimolecular kinetics, respectively
n_1, n_2 - Lower and upper wall slip parameters, respectively
$\overline{P}$ - Modified pressure (Pa)
P - Pressure (Pa)
Pr - Prandtl number
Q - Heat of reaction $(Wm^{-3}K^{-1})$
R - Universal gas constant $(Jmol^{-1}K^{-1})$
S - Porous medium shape parameter
T - Temperature (K)
T_a - Ambient temperature (K)
u - Dimensionless velocity component in the x-direction (ms^{-1})

Greek symbols

α - Variable viscosity parameter
α_1, β_3 - Material coefficients
β_0, β_1 - Lower and upper wall dimensional slip parameters
γ - Non-Newtonian parameter
δ - Material parameter
ε - Activation energy parameter
θ_a - Ambient temperature parameter
μ - Fluid dynamic viscosity (Pas)
λ - Frank-Kamenetskii parameter
ρ - Fluid density (kgm^3)

σ - Fluid electrical conductivity $(mhom^{-1})$
υ - Vibration frequency (Hz)
Ω - Viscous heating parameter

Acknowledgement

The authors are grateful to the anonymous referee for a careful checking of the details and for helpful comments that improved this paper.

References

[1] J. Hartmann, Theory of laminar flow of an electrically conducting liquid in a homogeneous magnetic field, Hg-Dynamics I, Math Fys Med, Vol. 15, pp. 1-28 (1737).
[2] S.O. Adesanya, E.O. Oluwadare, J.A. Falade and O.D. Makinde, Hydromagnetic natural convection flow between vertical parallel plates with time-periodic boundary conditions, Journal of Magnetism and Magnetic Materials, Vol. 396, pp. 295-303 (2015).
[3] H.A. Attia, Effect of Hall current on transient hydromagnetic Couette-Poiseuille flow of a viscoelastic fluid with heat transfer, Appl Math Modell, Vol. 32, pp. 375-388 (2008).
[4] H.A. Attia, Effect of porosity on unsteady Couette flow with heat transfer in the presence of uniform suction and injection, Kragujevac J Sci, Vol. 31, pp.11-16 (2009).
[5] A.J. Chamkha, On laminar hydromagnetic mixed convection flow in a vertical channel with symmetric and asymmetric wall heating conditions, Int J Heat Mass Transfer, Vol. 45, pp. 2509-2525 (2002).
[6] A.S. Idowu and J.O. Olabode, Unsteady MHD Poiseuille Flow between Two Infinite Parallel Plates in an Inclined Magnetic Field with Heat Transfer, IOSR Journal of Mathematics, Vol. 10, No. 3, pp. 47-53 (2014).
[7] J.K. Kwanza and J.A. Balakiyema, Magnetohydrodynamic Free convection flow past an Infinite Vertical Porous Plate with Magnetic Induction, J Fusion Energ, Vol. 31, No. 4, pp. 352-356 (2012).
[8] O.D. Makinde and A. Ogulu, The effect of Thermal Radiation on the Heat and Mass Transfer Flow of a variable Viscosity Fluid Past a Vertical Porous Plate Permeated by a Transverse Magnetic Field, Chem Eng Commun, Vol. 195, pp. 1575-1584 (2008).
[9] Sarveshanand and A.K. Singh, Magnetohydrodynamic free convection between vertical parallel porous plates in the presence of induced magnetic field, SpringerPlus, Vol. 4:333, pp. 1-13 (2015).
[10] K.G. Singha, Analytical solution to the problem of MHD free convective flow of an electrically conducting fluid between two heated parallel plates in the presence of an induced magnetic field, Int J Appl Math Comput, Vol. 1, No. 4, pp. 183-193 (2009).
[11] T. Hayat, S. Nadeem, A.M. Siddiqui and S. Asghar, An Oscillating Hydromagnetic Non-Newtonian Flow in a Rotating System, Applied Mathematics Letters, Vol. 17, pp. 609-614 (2004).
[12] Liu. I-Chung, Flow and heat transfer of an electrically conducting fluid of second grade over a stretching sheet subject to a transverse magnetic field, Int J Heat Mass Transfer, Vol. 47, pp. 4427-4437 (2004).
[13] O.D. Makinde, T. Chinyoka and L. Rundora, Unsteady flow of a reactive variable viscosity non-Newtonian fluid through a porous saturated medium with asymmetric convective boundary conditions, Comput Math Appl, Vol. 62, pp. 3343-3352 (2011).
[14] K.V. Prasad, P.S. Datti and K. Vajravelu, Hydromagnetic flow and heat transfer of a non-Newtonian power law fluid over a vertical stretching sheet, Int J Heat Mass Transfer, Vol. 53, pp. 879-888 (2010).
[15] K.R. Rajagopal, On Boundary Conditions for Fluids of the Differential Type: Navier-Stokes Equations and Related Non-Linear Problems, Plenum Press, New York, 1995.
[16] C. Truesdell and W. Noll, The non-linear field theories of mechanics, in: Fliigge (ED.), Handbuch der Physic, Springer, Berlin, 1965.
[17] B.I. Olajuwon, Convection heat and mass transfer in a hydromagnetic flow of a second grade fluid in the presence of thermal radiation and thermal diffusion, Int Commun Heat Mass Transfer, Vol. 38, pp. 377-382 (2011).
[18] H. Schlichting and K. Gersten, Boundary Layer Theory, McGraw-Hill, 1968.
[19] O.D. Makinde and T. Chinyoka, MHD transient flows and heat transfer of dusty fluid in a channel with variable physical properties and Navier slip condition, Comput Math Appl, Vol. 60, No. 3, pp. 660-669 (2010).
[20] M.T. Mathews and J.M. Hill, Newtonian flow with nonlinear Navier boundary condition, Acta Mech, Vol. 191, No. 3-4, pp. 195 (2007).
[21] Y.X. Zhu and S. Granick, Rate-dependent slip of Newtonian liquid at smooth surfaces-art, Phys Rew Lett, Vol. 8709, No. 9, pp. 6105 (2001).
[22] A.K. Al-Hadhrami, L. Elliot and D.B. Ingham, A new model for viscous dissipation in porous media across a range of permeability values, Transport in porous media, Vol. 53, pp. 117-122 (2003).
[23] D.A. Frank-Kamenetskii, Diffusion and Heat Transfer in Chemical Kinetics, Plenum Press, New York, 1969.
[24] O.D. Makinde, Hermite-Pade approximation approach to thermal criticality for a reactive third grade liquid in a channel with isothermal walls, Int Commun Heat Mass Transfer, Vol. 34, No. 7, pp. 870-877 (2007).
[25] M. Massoudi and I. Christe, Effects of variable viscosity and viscous dissipation on the flow of a third grade fluid in a pipe, Int J Nonlinear Mech, Vol. 30, pp. 687 (1995).
[26] M. Sajid, I. Ahmed, T. Hayat and M. Ayub, Unsteady flow and heat transfer of a second grade fluid over a stretching sheet, Commun Nonlinear Sci Numer Simul, Vol. 14, pp. 96-108 (2009).
[27] T. Chinyoka, Computational dynamics of a thermally decomposable visco-elastic lubricant under shear, Trans ASME J Fluids Eng, Vol. 130, No. 12,7.121201 (2008).
[28] T. Chinyoka, Poiseuille flow of reactive Phan-Thien-Tanner liquids in 1D channel flow, Trans ASME J Heat Transfer, Vol. 132, No. 11, 111701 (7 pages) (2010).
[29] T. Chinyoka, Suction-injection control of shear banding in non-isothermal and exothermic channel flow of Johnson-Segalman liquids, Trans ASME J Fluids Eng, Vol. 133, No. 7, 071205 (12 pages) (2011).

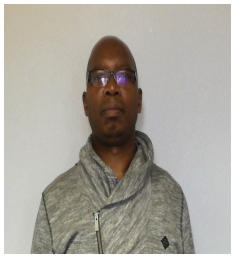

Lazarus Rundora received a Doctoral degree from Cape Peninsula University of Technology in South Africa. His research interests are in Fluid Mechanics, Heat and mass transfer, Mathematical modelling and Computational mathematics. He has published research articles in reputable international journals of Mathematical and Engineering Sciences. Lazarus Rundora is currently a senior lecturer in Mathematics at the University of Limpopo in South Africa. Prior to joining University of Limpopo, he lectured at University of Zimbabwe, Zimbabwe Open University and Vaal University of Technology. Lazarus Rundora is a reviewer of several international journals.

Oluwole Daniel Makinde is currently a Distinguished Professor of Computational and Applied Mathematics at the Faculty of Military Science, Stellenbosch University, South Africa. He is an Adjunct Professor at the Nelson Mandela African Institute of Science and Technology in Arusha-Tanzania; visiting Professor at the African University of Science and Technology in Abuja-Nigeria and visiting Professor at Pan African University Institute for Basic Science Technology and Innovation in Nairobi-Kenya. He received the PhD degree in Applied MathematicsFluid Mechanics at the University of Bristol (United Kingdom). He is a Fellow of African Academy of Sciences, Fellow of Papua New Guinea Mathematical Society. He won several prestigious academic research awards including: African Union Kwame Nkrumah Continental Scientific Award; South African TW Kambule Senior Researcher Award and Nigerian National Honour Award - Member of Order of the Federal Republic (MFR). He is a reviewer, editor and editorial board member of several international journals in the frame of Engineering Science, Applied Mathematics and Computations. His main research interests are: fluid mechanics, nanofluid dynamics, heat and mass transfer, hydrodynamic stability, mathematical modelling, computational mathematics, biomathematics and applications.